ORIGINAL ARTICLE

Construction of a three-dimensional model of renal stones: comprehensive planning for percutaneous nephrolithotomy and assistance in surgery

Hulin Li · Yuanbo Chen · Chunxiao Liu ·
Bingkun Li · Kai Xu · Susu Bao

Abstract

Objectives To construct a three-dimensional (3D) model of renal stones to facilitate comprehensive planning for percutaneous nephrolithotomy (PCNL) and to assist in surgery.

Methods Fifteen patients with complex renal stones, including one patient with a horseshoe kidney, eight patients with partial/complete staghorn, and six patients with multiple renal stones, participated in our study. Computed tomography images of the unenhanced, arterial, venous, and excretory phases were obtained before surgery. Image segmentation and 3D reconstruction of the renal stones were performed using Mimics 12.1 software. A virtual safe and reliable percutaneous renal access route were established for each patient by comprehensive planning based on the 3D model of renal stones. PCNL was subsequently performed with the assistance of the 3D model. Patient demographics, surgical details, and postoperative treatment parameters were recorded.

Results The 3D models of renal stones accurately represented the interrelationships between the intrarenal arteries and veins, collecting system, stones, and adjacent anatomical structures. PCNL was completed successfully in all 15 patients. The mean operating time was 75.6 ± 13.4 min. The change in hemoglobin concentration was 1.2 ± 0.3 g/l. The one-stage stone-free rate was 93.3 %, and the final stone-free rate was 100 %. No major postoperative complications were noted, except for postoperative pain in one case.

Conclusion Construction of a 3D model of renal stones with the aim of minimizing the risks of percutaneous procedures and achieving higher one-stage stone-free rates is feasible for comprehensive PCNL planning and assistance in patients with complex renal stones.

Keywords Complex renal stone · Three-dimensional model · Percutaneous nephrolithotomy · Comprehensive planning · Minimally invasive

Hulin Li and Yuanbo Chen contributed equally to this study and should be considered co-first authors.

H. Li · Y. Chen · C. Liu (✉) · B. Li · K. Xu
Department of Urology, Zhujiang Hospital of Southern Medical University, Guangzhou, Guangdong 510282, People's Republic of China
e-mail: liuchunx@hotmail.com

S. Bao
The Computer School, South China Normal University, Guangzhou, Guangdong 510631, People's Republic of China

Introduction

Percutaneous nephrolithotomy (PCNL) is the gold standard approach for managing large, multiple, or inferior calyx renal stones [1]. However, establishing an appropriate access route is challenging [2, 3], and it is a key to successful stone removal with minimal complications, especially for complex renal stones such as those in patients with a horseshoe kidney, staghorn calculi, or multiple renal stones. The risks of complications such as hemorrhage and injury to adjacent anatomical structures such as the pleura, colon, spleen, and liver are also high for PCNL for complex renal stones [4–7]. The best approach for managing these challenging cases is to remove the stones using the most minimally invasive procedure. We here suggest the novel approach of constructing a three-dimensional (3D) model of renal stones to facilitate comprehensive planning for PCNL and to assist in stone removal during surgery.

Patients and methods

From January to June 2012, 15 patients with complex renal stones (one patient with a horseshoe kidney, eight patients with partial/complete staghorn calculi, and six patients with multiple renal stones) who required PCNL were treated at our institution. Informed consent was obtained from all the patients, and the present study was approved by the Ethical Committee of Southern Medical University.

Construction of a three-dimensional (3D) model of renal stones

The patients were advised to lie in a prone position with the renal area of their abdomen on our PCNL cushion. Four-channel multi-detector row computed tomography (CT) images including the unenhanced, arterial, venous, and excretory phases were obtained using a 64 multi-detector row CT scanner (Philips, Brilliance 64, Netherlands) with 0.5-mm step intervals. The scan delay time for the arterial, venous, and excretory phases after intravenous injection of the contrast material was 25, 60, and 600–900 s, respectively. Image segmentation and 3D reconstruction were performed using Mimics 12.1 software (Materialise, Leuven, Belgium). The threshold value and manual division methods were combined and jointly interpreted by an experienced urologist and a radiology technician. The CT images from each patient were segmented by focusing on all aspects of the relevant structures including the renal parenchyma, intrarenal arteries, intrarenal veins, renal stones, the collecting system, spine, ribs, lungs, liver, spleen, and the skin on the back. All the 3D images were subsequently fused. The integrated 3D model of renal stones displayed all the related structures when the transparency was adjusted (Fig. 1).

Comprehensive planning for PCNL using a 3D model of renal stones

Preoperative PCNL planning was done by the surgeon using the simulation function in Mimics 12.1. The virtual 3D puncture needle was placed in the 3D model to mark the puncture channel. The simulation-reposition function, which includes the translation, rotation, and movement of the needle with a mouse, was used to control the planned puncture point and the direction of the needle in the 3D model in order to manage multiple stones simultaneously and to avoid damaging the intrarenal vasculature and adjacent anatomical structures. The 3D properties of the stones, such as the stone volume and surface area, were recorded using the Mimics 12.1 software [3]. The puncture depth (the depth of the puncture needle from the skin to the calyces), the horizontal distance between the planned puncture point and the median line of the spine, and the vertical distance to the 12th rib were also measured.

3D model used to assist with PCNL

The patients were placed in a prone position with the renal area of their abdomen on the PCNL cushion. This position was identical to that used during preoperative CT. The 3D model of the renal stones was displayed on one screen controlled by a surgical assistant on a separate computer. The needle insertion point was marked on the skin of the patients' back with reference to two lines marked in the 3D model: the horizontal distance between the planned puncture point and the median line of the spine and the vertical distance to the 12th rib (Fig. 2a). The image of the 3D model was zoomed in and rotated to display a 3D view of the planned puncture site (Fig. 2b). The real-time B ultrasound was adjusted; subsequently, the puncture line was manually marked on the ultrasound image by the surgeon on the basis of the 3D model view (Fig. 2c). The puncture needle was inserted from the needle insertion point marked on the patients' skin to the collecting system along the puncture line marked on the ultrasound image (Fig. 2d). During lithotripsy, the 3D model displayed the stones in the collecting system from various angles to provide more information on the anatomical structures. For each procedure, the operation time and the number of access ports were noted. The operation time was defined as the time
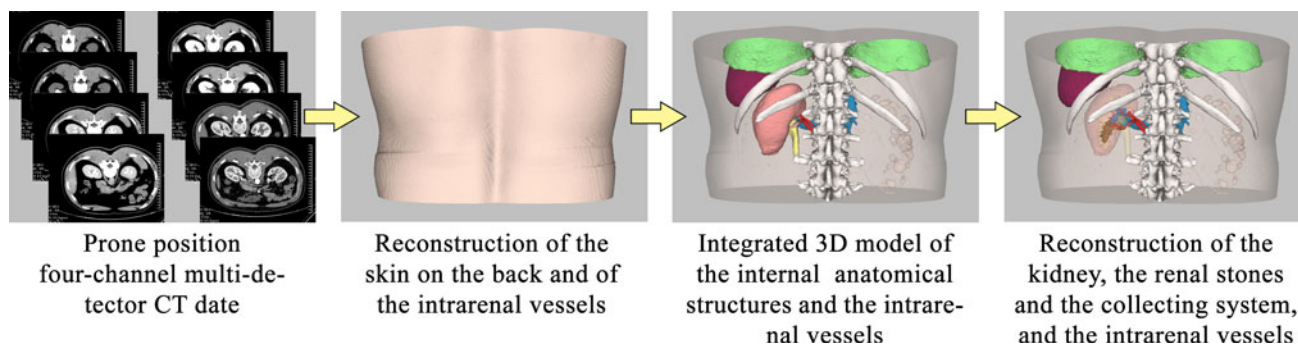

Fig. 1 Schematic of the process of creating an integrated three-dimensional model of renal stones

Prone position four-channel multi-detector CT date

Reconstruction of the skin on the back and of the intrarenal vessels

Integrated 3D model of the internal anatomical structures and the intrarenal vessels

Reconstruction of the kidney, the renal stones and the collecting system, and the intrarenal vessels
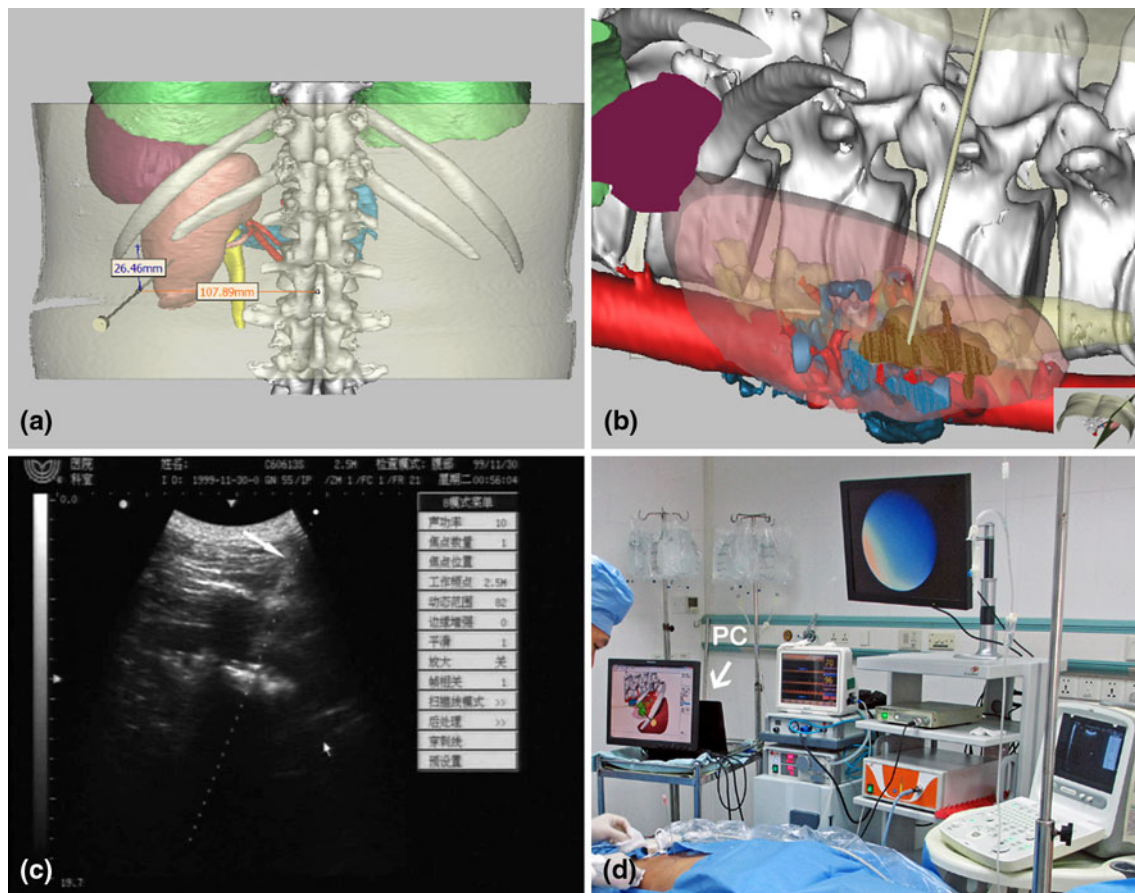
Fig. 2 Percutaneous nephrolithotomy performed under real-time B ultrasound guidance and with reference to the three-dimensional model

from the beginning of the needle puncture until the nephrostomy tube had been secured to the skin. Blood loss, blood transfusion rate, complication rate, and the number of stages required were also recorded. Blood loss was monitored by the postoperative decrease in hemoglobin levels and by the quantity of any blood transfusion. A kidney–ureter–bladder radiograph was used to monitor residual stone fragments on the first or second day after surgery and again after 2–4 weeks when the double J tube was removed. CT was used for radioparent stones. The stone-free rate was defined no any fragments >3 mm, which was accepted as clinically insignificant residual fragments [8, 9].

Results

Three-dimensional models of renal stones were constructed successfully for all 15 patients. The integrated 3D model of renal stones accurately represented the actual size of the kidney and its anatomical landmarks. By adjusting the transparency of the kidney, intrarenal arteries, veins, and collecting system with the stones were clearly visualized.

The number of stones, location of the collecting system, and dilation of the renal calyces were clearly visible. The interrelationships between the kidney and adjacent anatomical structures such as the spine, ribs, lungs, liver, and spleen were presented simultaneously. Preoperative comprehensive planning of PCNL was performed, and the puncture point and direction were planned before PCNL (Fig. 3).

With the aid of the 3D model, intraoperative PCNL was completed successfully in all 15 patients (Table 1). None of the patients required additional therapy. The mean stone volume was $11,591 \pm 6,889$ mm^3, the mean operating time was 75.6 ± 13.4 min, and blood loss was 1.2 ± 0.3 g/l. No intraoperative complications occurred. The one-stage stone-free rate was 93.3 %. One of the patients required a second stage to clear a residual 6-mm stone. Two patients required two tracts (one for a 20F sheath and the other for a 16F) to clear stones on the basis of their preoperative plans. The final stone-free rate was 100 %. No postoperative complications were noted, except for postoperative pain in one patient (Clavien grade 1).
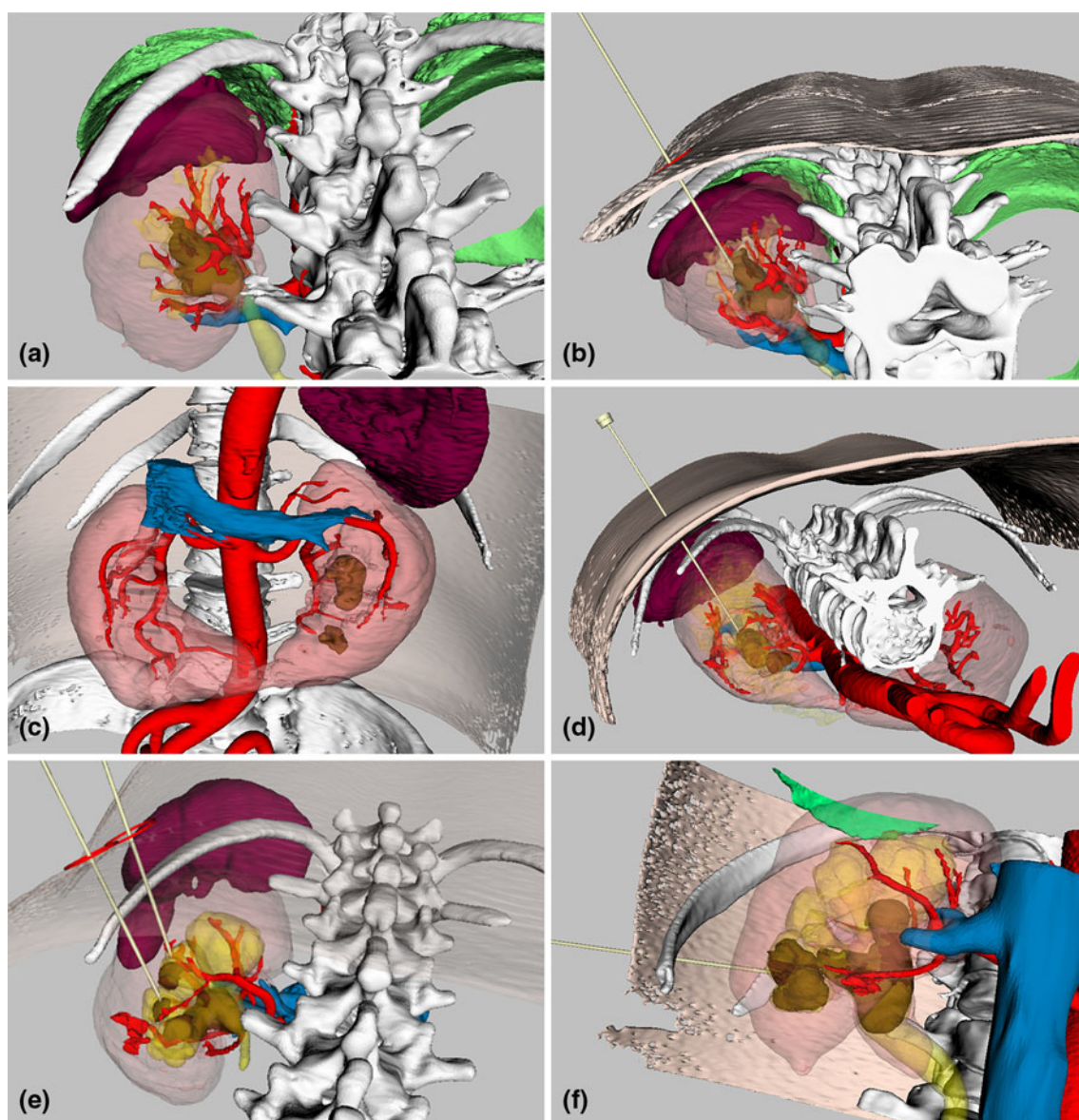
Fig. 3 Preoperative identification of the optimal percutaneous renal access route in the three-dimensional model of renal stones. **a**, **b**. Image of complete staghorn (volume, 7,525 mm³) in a right kidney. **c**, **d**. Image of a 5,906-mm³ volume renal stone in a left horseshoe kidney. **e**. Two percutaneous renal access routes were planned to remove multiple renal stones (volume, 4,466 mm³) in a left kidney. **f**. An 11th intercostal lower calyx access route was required to remove partial staghorn (volume, 15,876 mm³) in a right kidney

Discussion

Complex renal stones are a challenge during PCNL. A surgical puncture protocol is necessary for minimally invasive PCNL; therefore, PCNL in such cases is frequently performed using ultrasound or fluoroscopy-guided access. However, these only provide a two-dimensional, lower-resolution, and incomplete images of important anatomical structures. Detailed preoperative imaging can provide more information to aid selection of an optimal percutaneous approach. Three-dimensional CT reconstruction of the pelvicalyceal system (PCS) and stones provides a global overview that can aid such planning and selection [10–12]. A 3D view of the renal arterial system and the PCS can help avoid segmental arterial injury [13]. Imaging-guided surgery includes preoperative imaging and planning, intraoperative imaging, and tracking. The rapid development of imaging-guided surgery and the confirmation of its feasibility for urological applications [14–16] have led to intraoperative imaging being combined with preoperative planned imaging or the needle guidance systems for PCNL procedures. Novel procedures involving laser-guided percutaneous kidney

Table 1 Demographics and perioperative data for all 15 patients

Parameters	Mean ± SD or No. (%)
Demographics	
No. of patients	15
Age, year, mean ± SD	54.8 ± 8.8
Gender: male: female	8: 7
Body mass index, kg/m², mean ± SD	24.9 ± 2.0
Diabetes mellitus, no. (%)	2 (13.3)
Stone characteristics	
Stone side, n (%)	
Right	6 (40)
Left	9 (60)
Stone type	
Multiple renal stones, n (%)	6 (40)
Horseshoe kidneys, n (%)	1 (6.7)
Partial/Complete staghorn, n (%)	8 (53.3)
Stone surface area, mm², mean ± SD	3,723 ± 1,842
Stone volume, mm³, mean ± SD	11,591 ± 6,889
Perioperative	
Renal puncture site	
Upper pole, n (%)	4 (26.7)
Middle pole, n (%)	8 (53.3)
Lower pole, n (%)	3 (20)
Location of access	
Above 12th rib, n (%)	3 (20)
Below 12th rib, n (%)	12 (80)
Tract Requirement	
Single tract, n (%)	13 (86.7)
Two tract, n (%)	2 (13.3)
Stage requirement	
Single stage, n (%)	14 (93.3)
Two stage, n (%)	1 (6.7)
Operating time, min, mean ± SD	75.6 ± 13.4
Change in hemoglobin, g/dl, mean ± SD	1.2 ± 0.3
One-stage stone-free rate, n (%)	14 (93.3)
Final stone-free rate, n (%)	15 (100)
Blood transfusion rate, n (%)	0
Length of hospital stay, days, mean ± SD	5.0 ± 1.1
Complications, n (%)	1[a]

[a] Postoperative pain (Clavien grade 1)

access and iPad-assisted augmented reality have been found to be feasible for 3D puncture planning [17, 18], but there have been few clinical studies involving these applications. In our study, a 3D model that reconstructed the renal stones and associated anatomy of each patient was created using CT volume data; 3D reconstruction software (such as 3D Doctor and Mimics) is good for image segmentation [3, 19]. The reconstruction process is not so complex as is reported the similar 3D technique has demonstrated feasible in urinary surgical procedures [15, 18, 20]. Spatial errors in our study were minimized by ensuring similar positioning and respiration during the preoperative CT imaging and intervention. The reconstructed 3D model accurately represented the interrelationships between the intrarenal arteries and veins, the collecting system, and the stones, all of which could be visualized by adjusting the transparency of the kidney. The smallest avascular area was included in the design to avoid severe bleeding as the most severe bleeding is caused by segmental artery injuries [21, 22]. Munver et al. reported bleeding rates of 16 % for supracostal and 4.5 % for subcostal tracts [23]. The incidence of colonic, splenic, and liver perforations generally ranges from 0 to 0.4 % [6, 7]. An appropriate channel can be identified during preoperative planning to avoid injuring the adjacent anatomical structures, especially when an access point above the 12th rib is used. Our 3D model provided essential information for choosing the optimal percutaneous access for PCS.

The crucial procedure during PCNL is the puncture and dilatation of the tract to obtain proper renal access. Because of our 3D model, the puncture route was already planned, which promoted the cumbersome locating process easier. With rigid nephroscopy, it is difficult to remove some stones because of the acute angle of the kidney calyces. Although flexible nephroscopy has advantages in treating special cases [24, 25], it is too expensive for common use. An appropriate puncture channel is very helpful for rigid nephroscopy because it facilitates the management of multiple stones. An intraoperative panoramic view of the stone and collecting system provides more information than endoscopy, which promotes one-stage clearance of staghorn stones.

In our initial clinical experience, our 3D model of renal stones aided comprehensive planning for PCNL and assisted in surgery. Clearance was achieved for all 15 patients with complex stones. The one-stage stone-free rate was 93.3 %. The surgeon was also more confident and comfortable with the calyceal puncture because of the comprehensive preoperative planning.

The present study has some limitations. The patients were exposed to increased radiation because four-channel multi-detector CT rather than a conventional unenhanced CT scan was used. Extra time was required between image acquisition and the intervention. There was no real-time automatic fusion of images. Prospective comparative studies are required to confirm the value of this method. However, we present a new and effective method for managing complex stones. The 3D model of renal stones provided detailed information for comprehensive planning of PCNL and assisted in surgery. Furthermore, as the number of 3D models of complex stones reconstructed using this novel approach increase, a database of 3D stones can be developed to help train urology residents in PCNL.

Conclusions

We demonstrated that constructing a 3D model of renal stones is technically feasible for comprehensive PCNL planning and assistance in patients with complex renal stones. It can be recommended in patients with complex stones to minimize the risks associated with percutaneous procedures and to achieve higher one-stage stone-free rates.

Conflict of interest The authors have no conflict of financial interest to declare.

References

1. Al-Kohlany KM, Shokeir AA, Mosbah A, Mohsen T, Shoma AM, Eraky I, El-Kenawy M, El-Kappany HA (2005) Treatment of complete staghorn stones: a prospective randomized comparison of open surgery versus percutaneous nephrolithotomy. J Urol 173(2):469–473

2. Watterson JD, Soon S, Jana K (2006) Access related complications during percutaneous nephrolithotomy: urology versus radiology at a single academic institution. J Urol 176(1):142–145

3. Mishra S, Sabnis RB, Desai M (2012) Staghorn morphometry: a new tool for clinical classification and prediction model for percutaneous nephrolithotomy monotherapy. J Endourol 26(1):6–14

4. Turna B, Nazli O, Demiryoguran S, Mammadov R, Cal C (2007) Percutaneous nephrolithotomy: variables that influence hemorrhage. Urology 69(4):603–607

5. Muslumanoglu AY, Tefekli A, Karadag MA, Tok A, Sari E, Berberoglu Y (2006) Impact of percutaneous access point number and location on complication and success rates in percutaneous nephrolithotomy. Urol Int 77(4):340–346

6. de la Rosette J, Assimos D, Desai M, Gutierrez J, Lingeman J, Scarpa R, Tefekli A (2011) The clinical research office of the endourological society percutaneous nephrolithotomy global study: indications, complications, and outcomes in 5803 patients. J Endourol 25(1):11–17

7. El-Assmy AM, Shokeir AA, El-Nahas AR, Shoma AM, Eraky I, El-Kenawy MR, El-Kappany HA (2007) Outcome of percutaneous nephrolithotomy: effect of body mass index. Eur Urol 52(1):199–204

8. Tanriverdi O, Boylu U, Kendirci M, Kadihasanoglu M, Horasanli K, Miroglu C (2007) The learning curve in the training of percutaneous nephrolithotomy. Eur Urol 52(1):206–211

9. Jang WS, Choi KH, Yang SC, Han WK (2011) The learning curve for flank percutaneous nephrolithotomy for kidney calculi: a single surgeon's experience. Korean J Urol 52(4):284–288

10. Thiruchelvam N, Mostafid H, Ubhayakar G (2005) Planning percutaneous nephrolithotomy using multidetector computed tomography urography, multiplanar reconstruction and three-dimensional reformatting. BJU Int 95(9):1280–1284

11. Ghani KR, Rintoul M, Patel U, Anson K (2005) Three-dimensional planning of percutaneous renal stone surgery in a horseshoe kidney using 16-slice CT and volume-rendered movies. J Endourol 19(4):461–463

12. Soria F, Delgado MI, Sanchez FM, Allona A, Jimenez Cruz JF, Morell E, Uson J (2009) Effectiveness of three-dimensional fluoroscopy in percutaneous nephrostomy: an animal model study. Urology 73(3):649–652 discussion 652-644

13. Dalela D, Gupta A, Ahmed S, Goel A (2009) Three-dimensional synchronized multidirectional renal pyelo-angiography: a new imaging concept to facilitate percutaneous nephrolithotomy in technically challenging cases. J Endourol 23(12):1937–1939

14. Ukimura O (2010) Image-guided surgery in minimally invasive urology. Curr Opin Urol 20(2):136–140

15. Teber D, Guven S, Simpfendorfer T, Baumhauer M, Guven EO, Yencilek F, Gozen AS, Rassweiler J (2009) Augmented reality: a new tool to improve surgical accuracy during laparoscopic partial nephrectomy? Preliminary in vitro and in vivo results. Eur Urol 56(2):332–338

16. Simpfendorfer T, Baumhauer M, Muller M, Gutt CN, Meinzer HP, Rassweiler JJ, Guven S, Teber D (2011) Augmented reality visualization during laparoscopic radical prostatectomy. J Endourol 25(12):1841–1845

17. Ritter M, Rassweiler MC, Hacker A, Michel MS (2012) Laser-guided percutaneous kidney access with the Uro Dyna-CT: first experience of three-dimensional puncture planning with an ex vivo model. World J Urol [Epub ahead of print]

18. Rassweiler JJ, Muller M, Fangerau M, Klein J, Goezen AS, Pereira P, Meinzer HP, Teber D (2012) iPad-assisted percutaneous access to the kidney using marker-based navigation: initial clinical experience. Eur Urol 61(3):628–631

19. Mei J, Yin Z, Zhang J, Lui KW, Hu S, Peng Z, Chen S, Tang M (2010) A mini pig model for visualization of perforator flap by using angiography and MIMICS. Surg Radiol Anat 32(5):477–484

20. Ukimura O, Nakamoto M, Gill IS (2012) Three-dimensional reconstruction of renovascular-tumor anatomy to facilitate zero-ischemia partial nephrectomy. Eur Urol 61(1):211–217

21. Rastinehad AR, Andonian S, Smith AD, Siegel DN (2009) Management of hemorrhagic complications associated with percutaneous nephrolithotomy. J Endourol 23(10):1763–1767

22. Richstone L, Reggio E, Ost MC, Seideman C, Fossett LK, Okeke Z, Rastinehad AR, Lobko I, Siegel DN, Smith AD (2008) First Prize (tie): hemorrhage following percutaneous renal surgery: characterization of angiographic findings. J Endourol 22(6):1129–1135

23. Munver R, Delvecchio FC, Newman GE, Preminger GM (2001) Critical analysis of supracostal access for percutaneous renal surgery. J Urol 166(4):1242–1246

24. Walsh RM, Kelly CR, Gupta M (2009) Percutaneous renal surgery: use of flexible nephroscopy and treatment of infundibular stenoses. J Endourol 23(10):1679–1685

25. Williams SK, Leveillee RJ (2008) A single percutaneous access and flexible nephroscopy is the best treatment for a full staghorn calculus. J Endourol 22(9):1835–1837 discussion 1839